Selected for a Viewpoint in *Physics*

PHYSICAL REVIEW B **79**, 054515 (2009)

Experiments with single electrons in liquid helium

W. Guo, D. Jin, G. M. Seidel, and H. J. Maris
Brown University, Providence, Rhode Island 02912, USA

(Received 19 August 2008; revised manuscript received 31 October 2008; published 17 February 2009)

We describe experiments we have performed in which we are able to image the motion of individual electrons moving in liquid helium 4. Electrons in helium form bubbles of radius ~19 Å. We use the negative pressure produced by a sound wave to expand these bubbles to a radius of about 10 μm. The bubbles are then illuminated with light from a flash lamp and their position recorded. We report on several interesting phenomena that have been observed in these experiments. It appears that the majority of the electrons that we detect result from cosmic rays passing through the experimental cell. We discuss this mechanism for electron production.

DOI: 10.1103/PhysRevB.79.054515 PACS number(s): 67.25.dg, 13.85.Tp, 29.40.Mc

I. INTRODUCTION

In several previous experiments in our laboratory, the cavitation in liquid helium that results from nucleation at an electron bubble has been studied.[1–5] The energy E of an electron bubble of radius R in helium is given by the approximate expression

$$E = \frac{\hbar^2}{8m_e R^2} + 4\pi R^2 \alpha + \frac{4\pi}{3} R^3 P, \tag{1}$$

where the three terms represent the zero-point energy of the electron confined in a spherical cavity, the surface energy, and the work done against the applied pressure P in forming the cavity. α is the surface tension and m_e is the mass of the electron. The variation in the energy E with radius is shown in Fig. 1. At zero pressure the minimum energy is for a radius of 19 Å. For negative pressures, the radius increases and at a critical pressure P_c, the bubble becomes unstable against isotropic radial expansion and "explodes." P_c has the value[6]

$$P_c = -\frac{16}{5}\left(\frac{2\pi m_e}{5h^2}\right)^{1/4} \alpha^{5/4}. \tag{2}$$

In the low-temperature limit P_c has the value -1.9 bars; the magnitude of P_c decreases at higher temperatures due to the temperature dependence of α. This critical pressure is considerably smaller in magnitude than the pressure required to cause homogeneous nucleation of bubbles in helium. Consequently, cavitation due to electron bubbles is readily distinguished from cavitation due to homogeneous nucleation. In most of the experiments performed so far, a hemispherical transducer has been used to focus sound to a region in the liquid with a volume of the order 10^{-5} cm^3. If the pressure swing due to the sound pulse is large enough and if an electron bubble is in the focal region, cavitation will occur. In this type of measurement, a series of pulses is applied and the number of times that cavitation occurs is recorded. From an analysis of how the probability of cavitation varies with the driving voltage applied to the transducer, it is possible to deduce the pressure threshold P_c for cavitation and also the number density of the electron bubbles.

In the experiment that we report here[7] instead of using focused sound, we employ a planar ultrasonic transducer so as to produce a transient negative pressure over a large volume (~1 cm^3) of liquid helium 4. In this way, we explode all electron bubbles within the volume. By choosing a suitable ultrasonic frequency, we can make each bubble expand to a size that is sufficiently large that we can determine its position. Through the application of a series of sound pulses, we can then take images that show the track of individual electrons.

We first describe the design of the experiment (Sec. II). The main experimental challenge is the design of an ultrasonic transducer that can produce the required pressure swing throughout a large volume. In Sec. III we present results obtained. Some of the electron tracks that we see are believed to show the motion of electron bubbles that are trapped on quantized vortices and sliding along the vortices. Surprisingly, tracks of electron bubbles were observed in the liquid helium even when no electron source was installed in the cell. In most of the tracks an electron is first seen close to the surface of the sound transducer. We discuss the possible origin of these electrons in Sec. IV. We consider in detail a model in which the electrons are the results of cosmic rays passing through the liquid. Finally, we mention some pos-

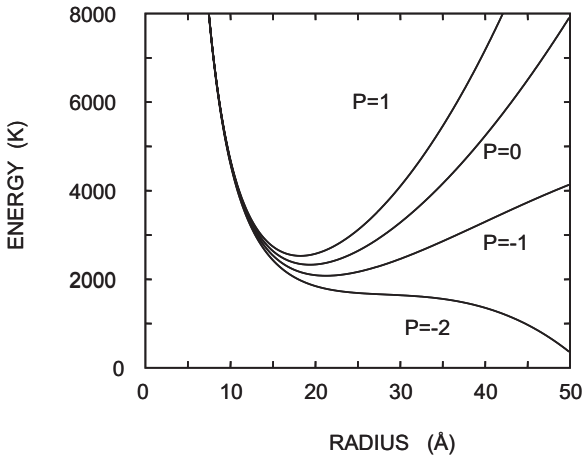

FIG. 1. Energy of an electron bubble as a function of radius. The curves are labeled by the pressure in bars.

sible applications of the imaging technique that has been developed. Monitoring the motion of single electron bubbles in liquid helium may have applications to the study of the flow of both normal and superfluid helium, to the study of quantized vortices, and to investigation of the exotic ions.

II. EXPERIMENT

A highly energetic electron passing through condensed matter will result in the excitation and ionization of atoms along its path. The track of the electron can be determined by observation of the scintillation from the excited atoms, or through the detection of the ionization produced in the material or the energy deposited.[8] For an electron that is moving slowly, these detection methods cannot be applied since the electron does not have enough energy to excite atoms. The determination of the position of an electron by optical means is extremely challenging because of the very small cross section for photon-electron scattering. For a free electron, the total scattering cross section is given by the Thomson cross section[9]

$$\sigma = \frac{8\pi}{3}\left(\frac{e^2}{mc^2}\right)^2 = 6.7 \times 10^{-25}\ \text{cm}^2. \tag{3}$$

This formula is valid if the photon energy is much less than the rest mass of the electron. If the electron is in a liquid or a solid there may be extra scattering because the presence of the electron modifies the medium around it and because the electron is no longer free. This modification is particularly pronounced for an electron in liquid helium. An electron strongly repels helium atoms because of the exclusion principle; the $1S$ levels of the helium atom are occupied and for another electron to be within the volume of the atom the electron has to go to a higher energy state with quantum number $n=2$. Furthermore, liquid helium is an extremely soft material which has a low surface tension and is easily deformed. As a result, when an electron enters liquid helium it forces open a cavity that is free of helium atoms and becomes trapped in this cavity forming an object usually referred to as an electron bubble. This bubble can move through the liquid and has been studied extensively primarily through measurements of its mobility.[10] The presence of the hole in the liquid (a region of different dielectric constant from that of the liquid) gives a total scattering cross section σ given by[11]

$$\sigma = \frac{128\pi^5}{3}\frac{R^6}{\lambda^4}\left(\frac{n^2-1}{2n^2+1}\right)^2, \tag{4}$$

where λ is the light wavelength in vacuum and n is the refractive index of the liquid. For red light this gives a cross section of the order of 10^{-23} cm^2.

In order to image the motion of electrons, a much larger scattering cross section is needed. One possibility is to use a photon energy that causes the electron to make a transition to an excited state within the bubble. For example, photons of wavelength around 10 μm can excite the electron from the ground state to the $1P$ state.[12,13] The cross section for this process is much larger,[14] i.e., of the order of 10^{-14} cm^2. The electron can return to the ground state by emitting a photon of wavelength around 30 μm.[15] It might be possible to detect these photons and in this way determine the position of an electron bubble. In the present experiments we have used an alternative approach based on ultrasonics.

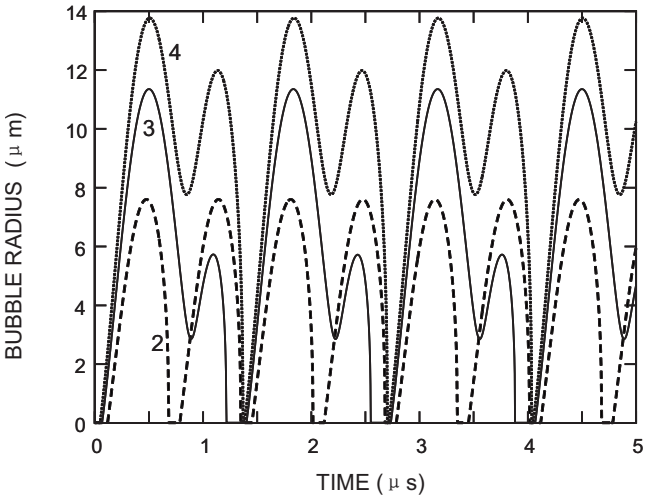

FIG. 2. Calculated radius of a bubble as a function of time based on Eq. (5). The different curves are labeled by the amplitude of the sound wave in bars.

We can enhance the scattering cross section of an electron bubble by increasing its size. If a negative pressure is applied to the bubble, the radius that minimizes the energy increases. At the critical pressure given by Eq. (2), the bubble becomes unstable, i.e., there is no value of the radius at which the energy has a minimum (see Fig. 1). Once the pressure becomes negative with respect to P_c, the bubble begins to grow very rapidly and can reach a large size. The radius of the bubble at a later time can be estimated by using the Rayleigh-Plesset equation[16]

$$\ddot{R} = -\frac{P(t)}{\rho R} - 3\frac{\dot{R}^2}{2R}, \tag{5}$$

where ρ is the density of the liquid. In the derivation of this equation, it is assumed that the work done by the negative pressure when the bubble expands is equal to the rate of increase in the kinetic energy of the liquid surrounding the bubble. Thus, the liquid is taken to be incompressible. The effect of the surface tension is neglected since surface tension is important only when the bubble is very small, i.e., when the radius is of the order of 1000 Å or less. To calculate the time dependence of the bubble radius for a given time dependence of the pressure produced by the sound, we take the bubble radius to be zero until the pressure drops below P_c. As an example, we show in Fig. 2 the radius as a function of time for a pressure varying as $P(t) = -P_0 \sin(2\pi ft)$, where P_0 is 2, 3 and 4 bars and the frequency is 1.5 MHz. In this figure, the nucleation pressure P_c is taken as -1.8 bars. For $P_0=2$ bars the maximum bubble radius $R_{\max}$ is 7.6 μm, and the bubble expands and collapses once each sound cycle. It follows from Eq. (5) that $R_{\max}$ is inversely proportional to the frequency f. Note that for

higher values of P_0, expansion and collapse takes place every two cycles of the applied sound instead of once per cycle.

As we will show in more detail below, it is possible to detect a bubble of radius ~ 10 μm by light scattering using a rather simple light source and detection scheme. Thus the combination of P_0 and $f=1.5$ MHz is adequate for the experiment, although a higher pressure would make detection easier. The greater challenge is to find an ultrasonic transducer capable of producing the required pressure swing. The amplitude of the pressure wave launched into bulk liquid by a planar transducer is given by the formula

$$\delta P_{\mathrm{He}} = \rho c v_{\mathrm{surface}}, \tag{6}$$

where c is the sound velocity in helium and v_{surface} is the velocity of the transducer surface. In order for δP_{He} to be 2 bars, the surface velocity has to be 600 cm s^{-1}. Consider a planar ultrasonic transducer with faces at $z=\pm w/2$. The acoustic impedance of liquid helium is much smaller than the impedance of the transducer material and so when the transducer vibrates the displacement is a maximum at the surface. Thus, in the lowest-order thickness mode the frequency is $f=c_{\mathrm{transducer}}/2w$ where $c_{\mathrm{transducer}}$ is the sound velocity in the transducer, and the displacement is $u(z)=u(d/2)\sin(\pi z/w)$. It follows that the strain in the transducer is

$$\eta(z) = \frac{v_{\mathrm{surface}}}{c_{\mathrm{transducer}}} \cos\left(\frac{\pi z}{w}\right). \tag{7}$$

Thus, the strain has a maximum value at the center of the transducer of $v_{\mathrm{surface}}/c_{\mathrm{transducer}}$. From this it follows that in order to have the required surface velocity the strain in the transducer has to be of the order of 10^{-3}, close to the breaking strain of many materials.[17] Operating the transducer in a higher order mode or using a transducer with a different thickness does not change the relation between the maximum strain and the surface velocity.

We have experimented with transducers of lead zirconate titanate, lead magnesium niobate-lead titanate,[18] and lithium niobate. It is not difficult to drive these transducers to achieve the required amplitude; the problem is that the transducers often break. We have had most success with 36° rotated y-cut $LiNbO_3$ with a frequency in the range 1.2 to 1.5 MHz.[19] In the first experiments a square plate was used with a side of 1.2 cm. The top and bottom surfaces of the transducer were plated with gold and electrical leads were soldered to the gold film. Because of the large acceleration of the surface ($\sim 6\times 10^9$ cm s^{-2}) the leads would often break off, sometimes pulling a piece of the transducer with them. To solve this problem we switched to circular transducers with cross section as shown in Fig. 3. The region near the edge of the transducer is tapered so that in this region the vibration amplitude is less than in the central part of the transducer. The electrical leads are soldered to the gold film in the tapered area. The lateral dimensions of the sound pulse should correspond to the 1.27 cm diameter of the part of the transducer that has the uniform thickness.

In order to obtain a high amplitude of the transducer without having to use a large driving voltage the transducer was typically driven at resonance for 30 μs. In order to minimize

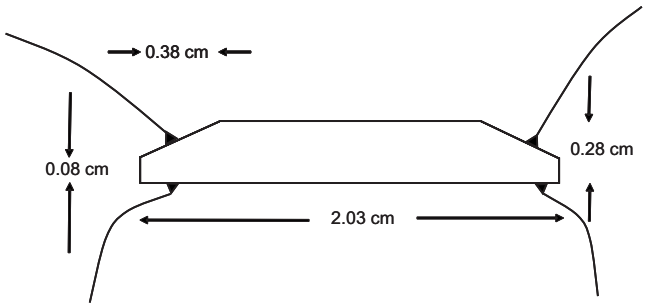

FIG. 3. Cross-sectional view of the lithium niobate ultrasonic transducer.

the chance of breaking the transducer, most observations were made with a driving voltage on the transducer no more than 10% above the minimum voltage needed to see exploded electron bubbles. Because the transducer was driven at a voltage greater than the minimum needed, and because its amplitude decreases slowly after the drive is turned off, it is likely that each sound pulse causes an electron bubble to explode several times but we have no way to verify this experimentally.

Two different experimental cells were used, each with windows for introducing light and for viewing the bubbles. These cells were installed in a ^{4}He optical cryostat with a 1 K pot. A sequence of sound pulses was applied with a repetition rate usually either 20 or 32 Hz. The electron bubbles were illuminated with light from a flash lamp; the timing of the light flashes was synchronized with the application of the sound pulses. The length of the sound path that could be viewed through the cell window was approximately 1 cm, and sound takes approximately 40 μs to cross this distance. Hence, to ensure that an exploded bubble would be illuminated no matter where it was when exploded, it was necessary to use sufficiently long light pulses. To reduce the amount of heat deposited in the cell by the flash, a mirror was placed inside the cell to reflect the light that passed through the helium back out toward the flash lamp. This also served to double the number of photons incident on the bubbles. Two different flash lamps were used and the time dependence of the output of each lamp was measured. From measurements of the total-energy output and allowing for geometrical factors, we estimate that the mean photon flux while the sound pulse traversed the cell was $\sim 2\times 10^{20}$ cm^{-2} s^{-1}.

The scattered light from the exploded bubble was recorded by a home-style camcorder[20] with its lens 15 cm from the center of the cell. The camcorder was placed at right angles to the incident light. A straightforward calculation using geometrical optics gives for the differential scattering cross section at this angle

$$\frac{d\sigma}{d\Omega} = \frac{R^2(n-1)^2}{4} \approx 2\times 10^{-4} R^2, \tag{8}$$

where n is the refractive index of liquid helium which has the value 1.028. This result is for unpolarized light and is correct to lowest order in $(n-1)$. For a bubble with radius 10 μm the differential scattering cross section is therefore only

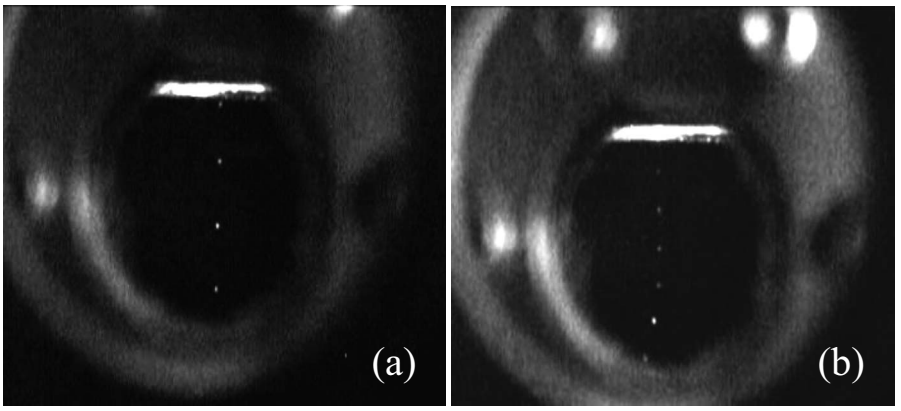

FIG. 4. Two images of an electron moving down the cell. The temperature is 1.5 K.

2×10^{-10} cm^2. As a result, it was important to keep other contributions to the scattered light to a minimum. The light from the flash lamp was collimated so that it did not contact the part of the cell wall that was viewed by the camcorder and all of the cell walls were painted black. The solid angle subtended by the camcorder lens was estimated to be 0.056 steradians and so the total number of photons reaching the camcorder was

$$N = 2 \times 10^{20} \times 0.056 \times 2 \times 10^{-4} \int R^2 dt, \qquad (9)$$

where the integral extends over the duration of the sound pulse. From the results for the bubble radius shown in Fig. 2, we find that the integral of R^2 over one cycle for a pressure oscillation of 2 bars is 2×10^{-13} cm^2. Thus, the number of photons is approximately 450 times the number of times n that the bubble explodes, so there are probably a few thousand photons reaching the camcorder for each sound pulse that is applied. With the available camera, we were able to detect these photons provided we used the camera in "super night mode" running at 4 frames/s with high sensitivity. Typically, if the acoustic pulses and flash lamp are set to run at 20 pulses/s, then as many as five positions of an electron are sometimes recorded by the camcorder on a single frame.

III. RESULTS

In the first few experiments, we used a cell attached to a continuously operating 1 K pot. The cell was cooled at the bottom and measurements could be made at temperatures down to 1.3 K. A planar lithium niobate transducer was mounted inside the cell at a height just above the top edge of the viewing window. The cell did not contain any source of electrons. The most commonly seen event is a single electron bubble moving from the top to the bottom of the cell. At 1.8 K the rate of seeing such electrons was measured to be 0.2 s^{-1}. Typical pictures are shown in Fig. 4. The bright bar in Fig. 4 at the top of the viewing window is the bottom surface of the transducer. As a first step, it was important to determine that the objects observed are in fact electrons. For example, one could suppose that the images come from the scattering of light by dust particles drifting around in the liquid. We were able to eliminate this possibility by looking to see if scattering occurred when the transducer was not excited. We found that there was no scattering. A second possibility is that the scattering arises more indirectly from dust particles in the liquid. The dust could be too small to give significant light scattering but might still be able to cause heterogeneous nucleation of bubbles in the presence of the sound wave. To test this we made measurements of how the number of times a scattering event was seen varied as a function of the voltage applied to the sound transducer. We observed a sharp threshold voltage below which almost no scattering could be observed. This sharp threshold is expected if we are seeing bubbles that grow from electron bubbles. For heterogeneous nucleation of bubbles on dust particles, however, we would expect that there would be a different pressure required for each particle and so there should be no sharp threshold. For higher voltages there is a slow increase in the probability of seeing electrons. We presume this is because the sound field falls off at the edge of the transducer and so when the transducer amplitude is increased, the volume within which electrons can be exploded increases.

The temperature dependence of the pressure needed to explode an electron bubble has been measured by Classen *et al.*[2] In that experiment the pressure was produced using a hemispherical transducer to bring sound to a focus. In Fig. 5, we compare those measurements with the measured voltage threshold in the current experiment. In order to make a best fit between the two data sets we have assumed that in the current experiment the pressure produced when 1 V is applied to the transducer is 0.002 bars. The agreement between the temperature dependence of the threshold as measured in the two experiments is reasonable.

The majority of the electrons that we have detected travel down the cell along smooth and slightly curved paths. They undergo this motion because of the drag exerted on the electron bubbles by the moving normal fluid. This normal fluid is the gas of thermally excited phonons and rotons and so we can consider that the electrons are drifting with the phonon-roton wind. The wind flows down the cell because the operation of the ultrasonic transducer results in a heat input at the top of the cell and this heat has to cross the cell in order to escape through the cooling heat link at the bottom. The velocity v_n of the normal fluid is given by

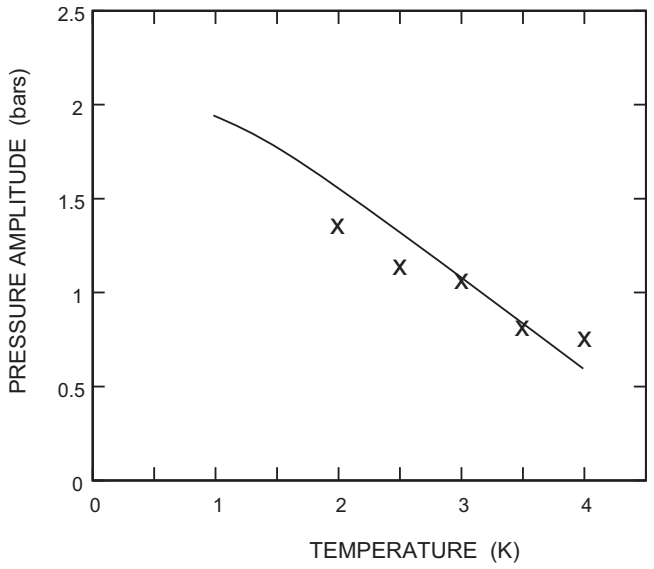

FIG. 5. Amplitude of the sound wave needed to explode an electron bubble as a function of temperature. The solid curve is the data of Classen *et al.* (Ref. 2) and the crosses are the present data.

$$v_n = \frac{\dot{Q}}{ATS}, \tag{10}$$

where A is the cross-sectional area of the cell and S is the entropy per unit volume. The velocity that we observe for the electrons is consistent with the velocity of the normal fluid as given by this formula when allowance is made for the fact that the cell does not have a simple geometry so the area A is not rigorously defined. As an example, Fig. 4(a) was obtained at 1.5 K, with an average power input to the transducer of ~250 mW. The measured electron velocity is about 5 cm s^{-1} and this is consistent with Eq. (10) if the area is taken to be 1 cm^2. Of course, an accurate calculation of the velocity of the normal fluid requires detailed allowance for the shape of the cell, the heat flow in the walls, and the Kapitza resistance. There may also be a contribution from acoustic streaming. The paths of the electrons tend to curve outward away from the center of the cell [see Fig. 4(b)]. This curvature occurs because the heat enters the fluid over a rather small area at the top of the cell whereas it leaves the cell over a larger area at the cell bottom.

The electron bubbles should also undergo a diffusive motion. The diffusion coefficient D is related to the mobility μ by the Einstein relation

$$D = \frac{\mu kT}{e}. \tag{11}$$

At 1.5 K, $\mu = 0.245$ cm^2 V^{-1} s^{-1} and so $D = 3.2 \times 10^{-5}$ cm^2 s^{-1}. The bubbles take about 1 s to drift from the top of the cell and so during this time move diffusively a distance that it is of the order of $\sqrt{Dt} \sim 0.006$ cm. This is too small for us to detect with the present apparatus.

A small fraction of the electrons that were seen first appeared at a point within the liquid helium far from the transducer surface. Examples are shown in Fig. 6. The rate of these events is about 0.04 s^{-1}. There are at least two possible origins of these electrons. They could result from cosmic rays, or other charged particles, that ionize helium atoms along a track. If a pair of the resulting positive and negative ions do not recombine this would result in an electron bubble appearing in the interior of the liquid. We will discuss this in more detail in Sec. IV. A second possibility is that the electron bubbles appear when a gamma from outside the helium, e.g., from the cell wall or other part of the cryostat, undergoes Compton scattering or photoelectric conversion within the helium. In a Compton scattering event, the recoil electron will usually have sufficient energy to travel far enough from the positive ion that recombination is unlikely to occur. Compton scattering lengths in liquid helium are 100 cm at 1 MeV, 40 cm at 100 keV, and 10 cm at 10 keV. Thus, for example, if we consider gammas of energy 100 keV, there would need to be a gamma flux of 0.16 cm^{-2} s^{-1} in order to give the number of electrons that we see first appear in the part of the interior of the cell through which sound travels and that we can observe, whereas for gammas of energy 1 MeV the flux would need to be 0.4 cm^{-2} s^{-1}. These rates are reasonable based on the results of a measurement of the integrated gamma background rate in the laboratory.[21] We have brought a ^{137}Cs gamma source of activity 10 μCi up to the outside of the cryostat and have seen that this increases the number of tracks that start in the liquid.

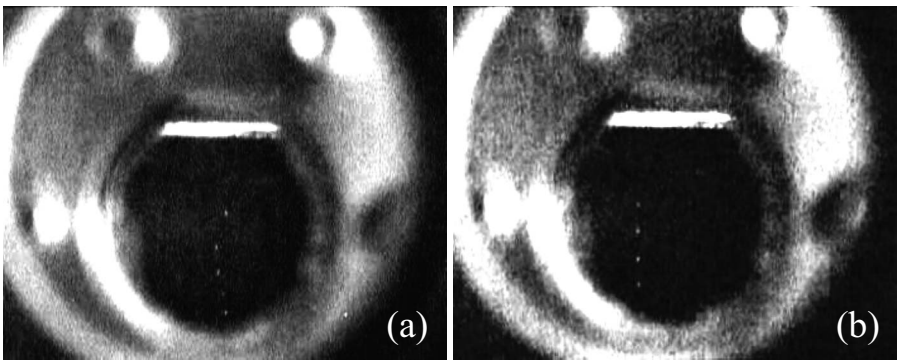

FIG. 6. Images in which an electron bubble is first seen at a point in the interior of the cell rather than near to the surface of the transducer. The temperature is 1.8 K.

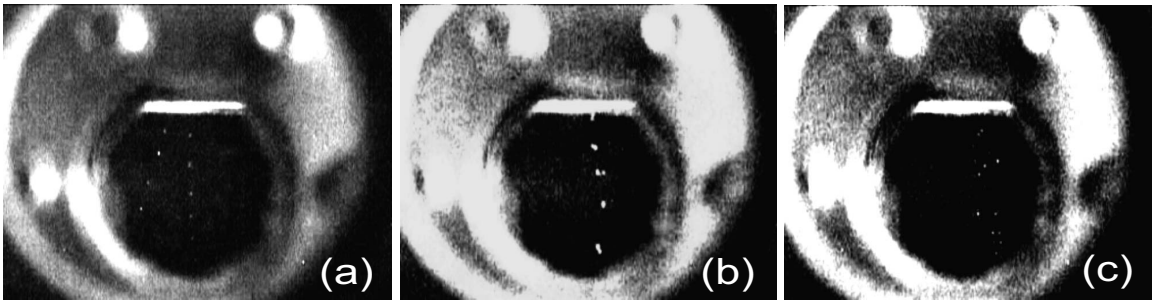

FIG. 7. Images in which more than one electron are seen. The temperature is 1.8 K.

In some of the images, two or more electrons are detected. This could just be a coincidence that two electrons enter the cell at the same time, but the number of times that this happens appears to be larger than would be expected on this basis. Examples are shown in Fig. 7. There appear to be different types of multielectron events. The most common (rate 0.03 s^{-1} at 1.8 K) are events in which two electrons appear to leave the surface of the transducer at the same time. Such an event is shown in Fig. 7(a). By extrapolating the paths of the two electrons backward in time, one can estimate when the electrons left the surface of the transducer. They appear to leave at the same time to within 2 ms and so it is unlikely that this is a coincidence. In Fig. 7(b), we show an event in which the two electrons originate a close distance apart and at the top of the cell. This is the only event we have seen like this and so we cannot assign an event rate for it. We have also seen events in which more than two electrons appear in the interior of the cell [Fig. 7(c)]. Although in this image there must be more than one electron present, it is not obvious which of the images are associated with which electron. One possibility is that these events originate when a first electron is excited by Compton scattering and then the lower energy gamma ray that is produced undergoes a second Compton scattering process or absorption by the photoelectric effect. We have also seen a few events in which an electron first appears in the interior of the cell along with an electron at the surface of the transducer.

In an attempt to make higher resolution recordings we increased the repetition rate of the sound pulses to 32 Hz. To improve the heat extraction from the cell, we moved the sound transducer to the bottom of the cell so that it was closer to the heat link to the 1 K pot. Despite making this change, it was no longer possible to keep the temperature below the lambda point. Below the lambda point the electrons should move with the normal-fluid component, and at a solid surface the velocity of this fluid should be normal to the surface. Above the lambda point the electrons should move with the classical fluid, and at the transducer surface the velocity of this fluid must be tangential to the surface although, of course, with the heat source at the bottom of the cell thermally driven convection will still result in a flow of liquid upward and away from the surface. Thus, a bubble leaving the surface should initially move laterally but then at some distance move primarily in the vertical direction. We have not been able to detect this type of motion, presumably because the change in the direction of the flow occurs near to the surface and we are only able to record the position of the electron every 31 ms. A set of images obtained with sound pulses at 32 Hz is shown in Fig. 8. In this experiment an electrode was placed at the top of the cell and a negative voltage applied to it. The convection of the liquid causes the electron to move in the vertical direction when it is close to the transducer but the path bends as the electron approaches the electrode.

Approximately 5% of the electrons that we see do not follow the smooth and slightly curved paths described so far. Instead, the electrons follow snakelike paths running from the top of the cell to the bottom (Here we are talking about the experiments below the lambda point with the transducer at the top of the cell). Two examples are shown in Fig. 9. At

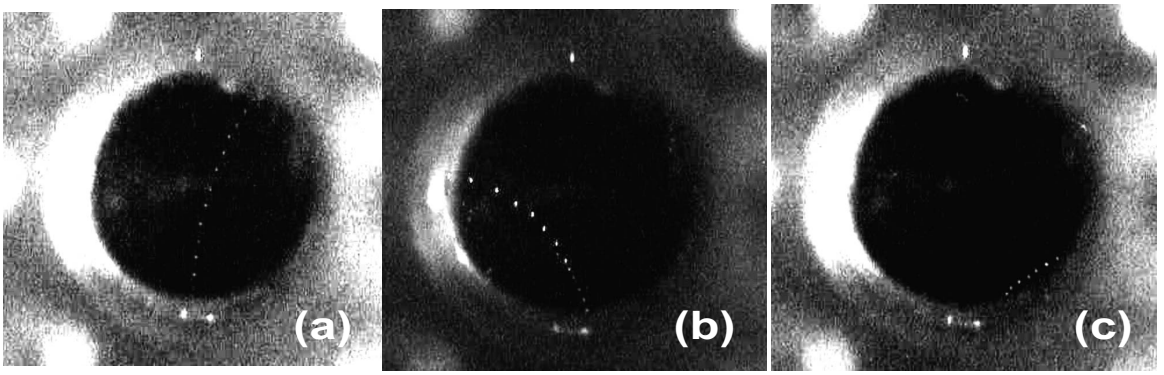

FIG. 8. Images of an electron moving under the combined influence of the upward convective flow of the liquid and an applied electric field. The electrode is at the bright spot at the top of the window. Voltage on the electrode is (a) 50, (b) 150, and (c) 500 V. The temperature is 2.4 K.

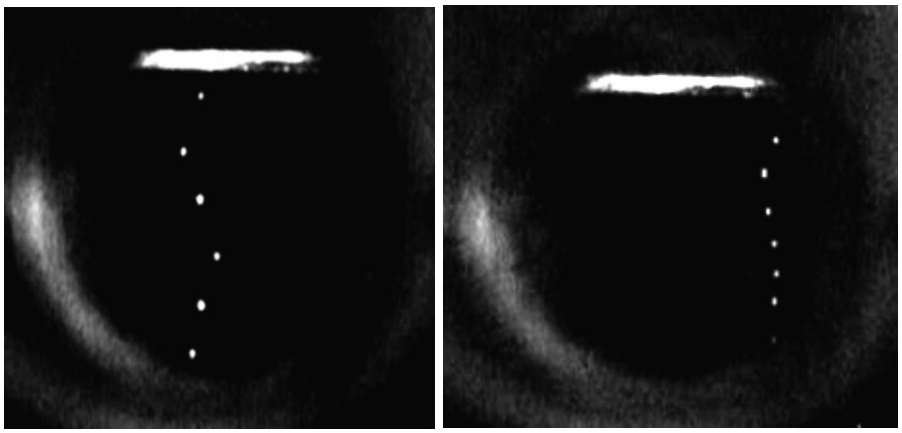

FIG. 9. Images of an electron following a snakelike track which may relate to the electron being trapped on and sliding along a vortex line. The temperature is 1.5 K.

first, we considered the possibility that this could arise from turbulence of the normal fluid but realized that this is impossible because these paths appear in the same volume of liquid as the other events. Instead, it appears that these tracks come from electrons that are trapped on quantized vortices. The superfluid circulating around the core of a vortex has a high velocity. An electron bubble positioned on a vortex line displaces liquid that has high kinetic energy and as a result there is an energy binding an electron to a vortex line.[22] Thus, an electron that becomes trapped on a line should follow the path of the line. The normal-fluid velocity in our experiments is typically 5 cm s^{-1} which is sufficient to result in the production of a tangle of vortices. According to Vinen's theory,[23] the vortex line density L_{eq} is given by

$$L_{eq} = (\alpha/\beta)^2 v_{ns}^2, \tag{12}$$

where α and β are Hall and Vinen's constants, and v_{ns} is the counterflow velocity. At 1.65 K, α/β is measured[24] to be 109 s cm^{-2}, and the counterflow velocity is nearly the same as the velocity of the normal fluid. Equation (12) then gives a line density of 3×10^5 cm^{-2}. The idea that vortices are responsible for the peculiar motion of the bubbles is supported by the observation that no such paths are seen above the lambda point. However, there are many open questions that we mention here briefly. (i) The potential holding the electron onto the vortex is short range, and it is remarkable that the bubble can grow to a radius of several μm and then return to its normal small size and still be attached to the vortex. (ii) It is not clear why we see only electrons that are attached to a vortex for the entire distance from the top of the cell to the bottom. It would seem more likely that we should see many tracks where an electron moves down freely for some distance and *then* becomes attached to a vortex, i.e., we should see tracks that are smoothly curved to begin with but then become snakelike. (iii) It is strange that the snake tracks that we see run almost straight down the cell; we never see snake tracks that run down at a large angle from the vertical. It is known that a vortex tangle is polarized (i.e., is not isotropic) by the flow of the normal fluid[25] but the polarization is such that there are more lines running perpendicular to the flow rather than parallel to it.[26]

Above about 1.7 K, electrons are able to escape from vortices,[27] and so above this temperature the snakelike paths should not be seen. We have not made a detailed study to determine the highest temperature at which these paths are detectable, but have found that they are not seen at 2 K.

Finally, we performed a simple experiment to visualize the sound field set up in the liquid by the transducer. We placed a 5 mCi ^{63}Ni beta source in the liquid. This produced a high density of electrons and an image of these electrons is shown in Fig. 10. One can see from the figure that the bubbles explode only in the region where the sound field is sufficiently strong.

IV. ORIGIN OF THE ELECTRONS

As already mentioned, no source of electrons was installed in the cell. We have considered the possibility that the observed electron bubbles appearing near the surface of the transducer are produced by cosmic rays passing through the cell. A high energy muon passing through the cell will cause ionization along its track. Most of the electrons knocked off

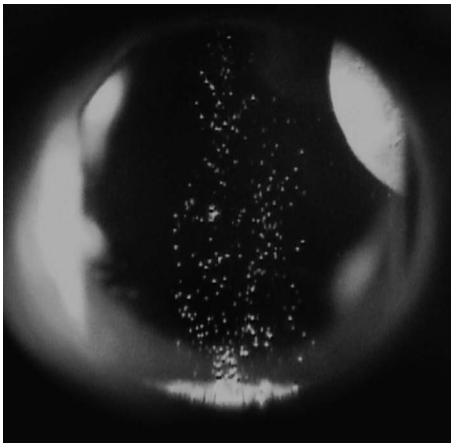

FIG. 10. Image taken when the cell contained a 5 mCi ^{63}Ni beta source in the liquid. The transducer is at the bottom of the cell. Only those electron bubbles that are in the sound field of the transducer explode.

of helium atoms will quickly recombine with the resulting positive ions, and only a small fraction of the electrons will escape. These electrons will be distributed uniformly throughout the cell. However, these cannot be the electrons that we are seeing since most of the electrons appear to start at the very top of the cell close to the surface of the transducer, rather than being distributed throughout the liquid. When the cosmic rays excite or ionize the helium, ultraviolet photons are produced. The energy of these photons is around 16 eV. We consider the possibility that when the uv photons reach the cell wall and the surface of the transducer, electrons are ejected into the helium by the photoelectric effect. At the bottom wall of the cell these electrons would be swept back into the wall by the normal fluid. We now consider this process quantitatively.

When passing through liquid helium, muons cause ionization and excitation of helium atoms. The average rate at which energy is deposited in liquid helium by a cosmic-ray muon is approximately 30 eV $\mu\mathrm{m}^{-1}$.[28] The ionization energy for helium is 24.6 eV. In pure helium gas the average energy to produce an electron-ion pair has been measured for an electron[29] to be $W=42.3\pm0.5$ eV and for an alpha particle[30] to be slightly larger, 43.3 ± 0.3 eV. It is reasonable to assume a comparable average energy needed for muons to produce an electron-ion pair. In helium the difference of 18 eV between the average energy of 43 eV to produce an electron-ion pair and the ionization energy of 24.6 eV goes into excitation of helium atoms and into kinetic energy of secondary electrons below the excitation threshold of 21.2 eV. Sato *et al.*[31] calculate that for every ion produced, 0.45 atoms are promoted to excited states. Of the excited atoms 83% are calculated to be in spin-singlet states and 17% in triplet states. The excited atoms, electrons, and ions quickly thermalize with the liquid helium. The electron, once thermalized, forms a bubble in the liquid typically within 4 ps.[32] The He^+ ion quickly forms a "helium snowball." The average distance between the electron bubble and its parent ion has been estimated by Benderskii *et al.*[33] to be 1000 Å. At 1000 Å spacing the Coulomb energy of the electron-ion pair is 170 K and, since this is much larger than kT, most electrons and ions in the liquid will quickly ($\sim10^{-11}$ s) recombine. At the experimental temperatures, most of the electron-ion pairs undergo geminate recombination in very short time ($\sim10^{-11}$ s). Experiments[34] indicate that roughly 50% of the excimers that form on recombination are in excited spin-singlet states and 50% are in spin-triplet states. These excited-state atoms, upon interacting with ground-state helium atoms, form diatomic excimer molecules

$$\mathrm{He}^* + \mathrm{He} \rightarrow \mathrm{He}_2^*. \tag{13}$$

A dimer in a highly excited singlet state can rapidly cascade to the first-excited state, $He_2(A^1\Sigma_u^+)$, and from there radiatively decay in less than 10^{-8} s to the ground state,[35] $He_2(X^1\Sigma_g)$, emitting an ultraviolet photon in a band from 13 to 20 eV and centered at 16 eV. For molecules in the triplet state $He_2(a^3\Sigma_u^+)$, however, the transition from the triplet state to the singlet ground state is forbidden since the transition involves a spin flip. The radiative lifetime of an isolated dimer in the triplet state $He_2(a^3\Sigma_u^+)$ has been measured[36] in liquid helium to be around 13 s. The triplet molecules can also be destroyed via a thresholdless bimolecular Penning ionization process[37] or quenching on the cell wall. In our experiments, due to the flow of the liquid, most of the triplet molecules generated when a cosmic-ray muon passes through the liquid will be dragged by the fluid and quenched on the cell wall before they can radiatively decay. Thus, we expect that only the singlet molecules will contribute to the number of ultraviolet photons produced in the cell. Based on the above analysis, the number of prompt ultraviolet photons per ion produced is then $0.5+0.45\times0.83=0.87$, the first term representing the fraction of ions that form singlet dimers on recombination and the second term accounting for the singlet dimers formed from excited atoms. These photons can pass through bulk helium because there is no absorption below 20.4 eV. A fraction of these photons will strike the surface of the transducer which is coated with gold. Given the work function of gold of 4.5 eV, photoelectrons can be emitted from the gold film into the liquid.

Considering the geometry of the cell used in our experiment, it is estimated that the flux of cosmic rays through the cell is roughly $\dot{N}_{\mathrm{cr}}\sim0.8/\mathrm{s}$.[38] The muons passing through different parts of the cell and at different angles have different track lengths in the liquid. For simplicity, here we take the average distance that each cosmic muon passes in the cell to be 7 cm. The total number of ultraviolet photons generated per cosmic-ray event N_{ph} is then approximately

$$N_{\mathrm{ph}} = \frac{30(\mathrm{eV}/\mu\mathrm{m})\times 7\ \mathrm{cm}}{43\ \mathrm{eV}} \times 0.87 = 4.2\times10^4. \tag{14}$$

Considering the solid angle of the transducer, we estimate that about 5% of the ultraviolet photons will reach the surface of the transducer. Hence the number of photons that strike the transducer per cosmic-ray event is roughly $N_{\mathrm{event}}=2.1\times10^3$. Let the probability that a photon striking the transducer produces an electron that escapes into the liquid helium be γ. Then the average rate of seeing electrons is

$$R_{\mathrm{el}} = N_{\mathrm{cr}}N_{\mathrm{event}}\gamma = 1700\gamma\ \mathrm{s}^{-1}. \tag{15}$$

Experimentally, the average rate of seeing electron bubbles appearing from the transducer is 0.2 events/s. As a result, we find that the photon-electron conversion probability is $\gamma\simeq1.1\times10^{-4}$.

As will be discussed below it is difficult to make an independent estimate of the value of γ, and consequently we have looked for another way to test this model. When the 16 eV photons strike the transducer surface, there is a finite probability that two electrons will be knocked out simultaneously. We can compare this rate with the rate expected based on the muon model just described, and use this as a consistency check of the model. The rate of the double-track events is given by

$$R_{\mathrm{el}}^{(2)} = \frac{N_{\mathrm{event}}(N_{\mathrm{event}}-1)}{2}\gamma^2(1-\gamma)^{N_{\mathrm{event}}-2}N_{\mathrm{cr}} = 0.017\ \mathrm{s}^{-1}. \tag{16}$$

This is in reasonable agreement with the observed double-track event rate of 0.03 s^{-1} considering the uncertainties in the geometry.

Is the value that we have found for γ reasonable? This involves a number of issues. We have been unable to find a measurement of the photoelectric efficiency for gold at 16 eV; we have found data up to 11 eV (Ref. 39) and above 20 eV.[40] In addition, the efficiency appears to be very dependent on the condition of the surface. The efficiency at 11 eV was found to be between 0.002 and 0.02 depending on the film thickness which varied from 75 to 240 Å. These values are for photoemission when the light was applied on one side of a gold film and the electrons were emitted from the other side. Efficiency is defined as the number of electrons emitted per incident photon. At 20 eV measurements were made on a gold film of thickness 1000 Å, and the efficiency was found to be 0.06. We do not know the thickness of the gold film on the transducer. Based on these limited data, we will take the efficiency to be 0.02 but this could certainly be incorrect by a factor of 2. We now have to consider what fraction f_{gold} of the electrons that leave the gold surface will escape into the bulk helium. This fraction is small because the emitted electrons are strongly scattered once they are in the helium and when they have lost their initial kinetic energy the positive image charge in the gold film pulls them back out of the liquid. However, the value of f_{gold} is increased because the flow of the normal fluid provides a drag force pulling electrons away from the gold film. We have performed Monte Carlo computer simulations to estimate f_{gold}. We assume that the mean distance from the gold surface at which an electron forms a bubble is ξ. Since the electron makes many collisions and undergoes a random walk, it is reasonable to assume that the distribution of final positions is a Gaussian. Then the probability that the electron travels a distance between r and $r+dr$ is

$$\frac{32}{\pi^2\xi^3}\exp(-4r^2/\pi\xi^2)r^2dr, \tag{17}$$

and the probability that the distance of the bubble from the surface of the gold film is between z and $z+dz$ is[41]

$$\frac{4dz}{\pi\xi}\exp(-4z^2/\pi\xi^2). \tag{18}$$

We then consider an electron bubble starting at some value of z. The combined effect of the motion of the normal fluid and the force due to the image charge gives the bubble a velocity along the z direction which is

$$v = -\frac{e\mu}{4z^2} + v_n, \tag{19}$$

where μ is the mobility. The bubble also undergoes a random motion given by the diffusion coefficient D, related to μ by the Einstein relation. We then consider an ensemble of 100 000 such bubbles with starting z coordinates distributed according to Eq. (18), and find the probability that a bubble can escape to a large positive value of z. Since f_{gold} is rather small it is necessary to consider a large ensemble. Results for 1.8 K are shown in Fig. 11 for velocities of the normal fluid of 2, 5, and 10 cm s^{-1}. In our experiments at 1.8 K, the normal-fluid velocity is usually close to 5 cm s^{-1}.[42]

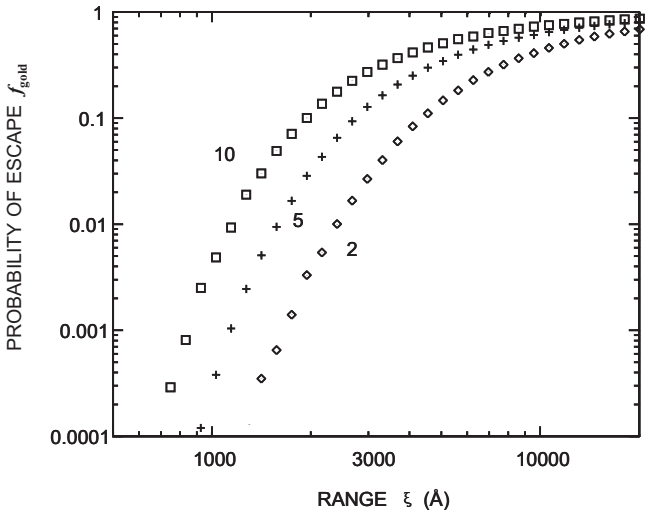

FIG. 11. Results of a computer simulation of the escape probability f_{gold} from the gold film on the transducer as a function of the mean range of the photoejected electrons. The different curves are labeled by the velocity of the normal fluid in cm s^{-1}. The simulations are for a temperature of 1.8 K.

To explain the measured value of γ we need the parameter f_{gold} to have a value of $1.1\times10^{-4}/0.02=5.5\times10^{-3}$. From Fig. 11, we see that for this to happen the average range ξ has to be 1430 Å. Benderskii *et al.*[33] have estimated the mean range by considering the number of elastic collisions an electron must make with helium atoms before the energy becomes low enough for the electron to be trapped in a bubble. They found a range of 1000 Å and this is in reasonable agreement with our result.[43]

Note that in our simulation we have considered the electron bubble to undergo a diffusive motion, i.e., the inertia of the moving bubble is not taken into account. The drag force on an electron bubble when it is moving with a velocity v is ev/μ. Hence the time for an initial velocity of an electron bubble to be lost is $\tau_{\text{inertia}}=M\mu/e$, where M is the hydrodynamic mass of the bubble. We can compare this time with the time τ_{fall} it takes a bubble to fall back to the positive ion under the influence of the Coulomb attraction. This time is of the order of $r^3/e\mu$ where r is the starting distance from the positive ion. Thus, the simulations should be valid when $\tau_{\text{inertia}} \ll \tau_{\text{fall}}$, i.e., when $\mu \ll \sqrt{r^3/M}$. For $r=1000$ Å, this condition gives $\mu \ll 2.3$ cm^2 V^{-1} s^{-1}. At 1.8 K the mobility of an electron bubble[44] is 0.11 cm^2 V^{-1} s^{-1} so this condition is well satisfied. μ becomes equal to $\sqrt{r^3/M}$ at around 1 K.

We now consider the experimental observation that we do *not* see a large number of electrons first appearing in bulk liquid. Based on the known muon flux,[38] we estimate that within the volume of the helium that we can observe and which sound passes through there should be 7×10^3 atoms ionized per second. This compares with the observed rate of electron bubbles appearing within this volume of 0.04 s^{-1}. Thus, the probability f_{ion} that an electron knocked off of a helium atom forms an electron bubble that does not recombine with the positive ion must be less than 6×10^{-6}. When a muon ionizes a helium atom in bulk liquid, both the positive ion and the electron will be dragged with equal velocity by

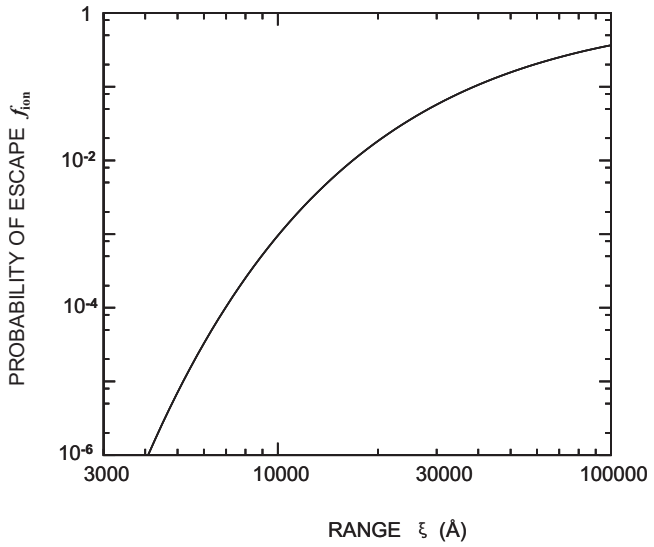

FIG. 12. Calculated escape probability f_{ion} of an electron bubble from a positive ion as a function of the mean range of the electron. The calculation is for a temperature of 1.8 K.

the normal fluid. Thus, the motion of the normal fluid has no effect on the probability that the electron can escape. In the measurement of the rate of appearance of electron bubbles in the bulk liquid no electric field was applied. The Coulomb attraction between the electron and the positive ion will cause both to move and so, at first sight, it would appear that the result for the escape probability should depend on the mobility of both objects. In fact, because of the Einstein relation connecting diffusion and mobility, the escape probability is a function of the single parameter $\xi kT/e^2$; the mobility only affects the time for escape or recombination to occur. For the case that the initial separation of the positive and negative ion is r, the escape probability is $\exp(-e^2/rkT)$ (Refs. 45 and 46) and so the mean escape probability is

$$f_{\text{ion}} = \frac{32}{\pi^2 \xi^3} \int_0^\infty \exp(-4r^2/\pi\xi^2)\exp(-e^2/rkT)r^2 dr, \quad (20)$$

f_{ion} as a function of ξ for $T=1.8$ K is shown in Fig. 12. In order for the escape probability to be less than 6×10^{-6} the mean range needs to be less than about 4900 Å. One expects that the energy of the electrons produced by muons will be larger than the energy for the electrons photoemitted from the gold surface (these have energy less than 12 eV). However, as has been pointed out by Benderskii *et al.*,[33] the mean range is expected to vary as the logarithm of the electron energy and so it is very unlikely that the range of the electrons produced by the muons is as great as 4900 Å.[47] As a result, we conclude that it is unlikely that the electrons bubbles that are detected in the bulk come from cosmic rays, and that they are probably the result of background gamma radiation.

V. SUMMARY

The purpose of this paper is to describe an apparatus which can be used to monitor the motion of individual electrons in liquid helium, to present images obtained using this apparatus, and to describe the mechanism for production of the electrons. A sound wave is used to explode an electron bubble for a fraction of a microsecond. While the bubble is expanded, it is illuminated by light from a flash lamp and imaged by a camera. Through the application of a series of sound pulses, we can then record the tracks of individual electrons. Some of the tracks are suspected to be related to bubbles being trapped on quantized vortices and sliding down the vortices. We have developed a model of electron production in which photons produced as a result of the passage of cosmic rays through the cell lead to photoemission of electrons into the helium. This model appears to be able to explain the rate of electron production and the occasional appearance of two electrons at the same time.

These experiments open up several new possibilities for the study of superfluid helium. Through the use of an electron source, (a β-source, for example), it should be possible to cause a large number of electrons to become attached to each vortex in the liquid. By exploding all of these electrons with a single sound pulse, it would then be possible to obtain a snapshot of the topology of the vortices. Since only a single sound pulse would be required, it should be possible to do this even down to temperatures considerably below 1 K. It should also be possible to use the technique to learn more about the mysterious "exotic ions.[48]" These are negative ions that appear to be smaller than ordinary electron bubbles. The physical nature of these objects is unknown, but which can presumably also be exploded by sound waves of sufficient amplitude.

ACKNOWLEDGMENTS

We thank Dmitri Feldman for helpful discussions. This work was supported in part by the National Science Foundation through Grant No. DMR-0605355.

[1] J. Classen, C. K. Su, and H. J. Maris, Phys. Rev. Lett. **77**, 2006 (1996).
[2] J. Classen, C.-K. Su, M. Mohazzab, and H. J. Maris, Phys. Rev. B **57**, 3000 (1998).
[3] D. Konstantinov and H. J. Maris, Phys. Rev. Lett. **90**, 025302 (2003).
[4] A. Ghosh and H. J. Maris, Phys. Rev. Lett. **95**, 265301 (2005).
[5] A. Ghosh and H. J. Maris, Phys. Rev. B **72**, 054512 (2005).
[6] V. A. Akulichev and Y. Y. Boguslavskii, Sov. Phys. JETP **35**, 1012 (1972).
[7] A preliminary report of this experiment has been given in W. Guo and H. J. Maris, J. Low Temp. Phys. **148**, 199 (2007).
[8] For the development of the bubble chamber and theoretical discussion, see D. A. Glaser, Phys. Rev. **87** 665 (1952); and

Phys. Rev. **91**, 762 (1953); F. Seitz, Phys. Fluids **1**, 2 (1958); A. G. Tenner, Nucl. Instrum. Methods **22**, 1 (1963).
[9] See, for example, W. Heitler, *The Quantum Theory of Radiation* (Oxford, New York, 1954).
[10] The properties of ions in helium have been reviewed by A. L. Fetter in *The Physics of Liquid and Solid Helium*, edited by K. H. Benneman and J. B. Ketterson (Wiley, New York, 1976); R. J. Donnelly, *Experimental Superfluidity* (University of Chicago Press, Chicago, 1967).
[11] H. C. van de Hulst, *Light Scattering by Small Particles* (Wiley, New York, 1957), p. 70.
[12] C. C. Grimes and G. Adams, Phys. Rev. B **41**, 6366 (1990).
[13] C. C. Grimes and G. Adams, Phys. Rev. B **45**, 2305 (1992).
[14] H. J. Maris and W. Guo, J. Low Temp. Phys. **137**, 491 (2004).
[15] H. J. Maris, J. Low Temp. Phys. **132**, 77 (2003).
[16] J. W. Strutt, Philos. Mag. **34**, 94 (1917); for attempts to improve the Rayleigh-Plesset equation to allow for the compressibility of the liquid, see T. G. Leighton, *The Acoustic Bubble* (Academic, New York, 1994), p. 307.
[17] The maximum strain was given incorrectly as 10^{-4} in the preliminary report.
[18] H.C. Materials, Bolingbrook, Illinois 60440, USA. For data on the low-temperature properties of this material, see W. Guo, D. Jin, W. Wei, H. J. Maris, J. Tian, X. Huang, and P. Han, J. Appl. Phys. **102**, 084104 (2007).
[19] Boston Piezo-optics, Bellingham, Massachusetts, USA.
[20] Sony model TRV 740 camcorder.
[21] We thank R.E. Lanou for providing us with the results of this measurement.
[22] See, for example, R. J. Donnelly, *Experimental Superfluidity* (Chicago, London, 1967).
[23] W. F. Vinen, Proc. R. Soc. London, Ser. A **240**, 114 (1957); **240**, 128 (1957); **242**, 493 (1957); **243**, 400 (1958).
[24] M.v. Schwerdtner, G. Stamm, and D. W. Schmidt, Phys. Rev. Lett. **63**, 39 (1989).
[25] K. W. Schwarz, Phys. Rev. B **38**, 2398 (1988).
[26] There have been several studies of vortices in cold Bose and Fermi gases, starting with the work of M. R. Matthews, B. P. Anderson, P. C. Haljan, D. S. Hall, C. E. Wieman, and E. A. Cornell, Phys. Rev. Lett. **83**, 2498 (1999); in helium the positions of the ends of an array of vortices were first observed by E. J. Yarmchuk, M. J. V. Gordon, and R. E. Packard, *ibid.* **43**, 214 (1979); very recently, G. P. Bewley, D. P. Lathrop, and K. R. Sreenivasan, Nature (London) **441**, 588 (2006) have succeeded in decorating vortices with small particles of solid hydrogen.
[27] See, for example, the review by R. J. Donnelly, *Quantized Vortices in Helium II* (Cambridge, Cambridge, 1991).
[28] The energy loss of high energy muons has been measured to be approximately 2 MeV g^{-1} cm^2, C. A. Ayre, M. A. Hamdan, C. J. Hume, M. G. Thompson, S. C. Wells, M. R. Whalley, and A. W. Wolfendale, J. Phys. A **4**, L75 (1971).
[29] W. P. Jesse and J. Sadauskis, Phys. Rev. **97**, 1668 (1955).
[30] See N. Ishida, J. Kikuchi, and T. Doke, Jpn. J. Appl. Phys. Part 1 **31**, 1465 (1992) and references therein.
[31] S. Sato, K. Okazaki, and S. Ohno, Bull. Chem. Soc. Jpn. **47**, 2174 (1974).
[32] J. P. Hernandez and M. J. Silver, Phys. Rev. A **2**, 1949 (1970).
[33] A. V. Benderskii, R. Zadoyan, N. Schwentner, and V. A. Apkarian, J. Chem. Phys. **110**, 1542 (1999).
[34] J. S. Adams, Ph.D. thesis, Brown University, 2001.
[35] M. Stockton, J. W. Keto, and W. A. Fitzsimmons, Phys. Rev. A **5**, 372 (1972).
[36] D. N. McKinsey, C. R. Brome, J. S. Butterworth, S. N. Dzhosyuk, P. R. Huffman, C. E. H. Mattoni, J. M. Doyle, R. Golub, and K. Habicht, Phys. Rev. A **59**, 200 (1999).
[37] J. W. Keto, F. J. Soley, M. Stockton, and W. A. Fitzsimmons, Phys. Rev. A **10**, 872 (1974).
[38] L. N. Bogdanova, M. G. Gavrilov, V. N. Kornoukhov, and A. S. Starostin, Phys. At. Nucl. **69**, 1293 (2006).
[39] W. Pong, R. Sumida, and G. Moore, J. Appl. Phys. **41**, 1869 (1970).
[40] R. H. Day, P. Lee, E. B. Saloman, and D. J. Nagel, J. Appl. Phys. **52**, 6965 (1981).
[41] This formula is an approximation since it includes in the probability of arriving at a distance z from the transducer all possible random walks starting at $z=0$. In a more accurate calculation paths in which at any point the electron has a negative z-coordinate should be excluded.
[42] In our simulation we consider the electron bubble to undergoing a diffusive motion, i.e., the inertia of the moving bubble is not taken into account.
[43] Earlier estimates of the range of electrons in helium by D. G. Onn and M. Silver [Phys. Rev. **183**, 295 (1969) and Phys. Rev. A **3**, 1773 (1971)] gave a result of around 100 Å. However, their measurements were for electrons of energy around 1 eV.
[44] R. J. Donnelly and C. F. Barenghi, J. Phys. Chem. Ref. Data **27**, 1217 (1998).
[45] L. Onsager, Phys. Rev. **54**, 554 (1938).
[46] K. M. Hong and J. Noolandi, J. Chem. Phys. **68**, 5163 (1978).
[47] The passage of a high energy charged muon through helium will result in a small number of ionization events in which unusually high energy electrons are produced; these are called delta rays. However, based on the range estimates of Benderskii *et al.* (Ref. 33), in order for a delta ray to have a range of 3000 Å, the energy would have to be very high and the rate of production of such delta rays is very small.
[48] G. G. Ihas and T. M. Sanders, Phys. Rev. Lett. **27**, 383 (1971); V. L. Eden and P. V. E. McClintock, Phys. Lett. **102A**, 197 (1984); C. D. H. Williams, P. C. Hendry, and P. V. E. McClintock, Jpn. J. Appl. Phys. **26**, Suppl. 26-3, 105 (1987).